VIP *Very Important Paper*

Pyridine Complexes as Tailored Precursors for Rapid Synthesis of Thiophosphate Superionic Conductors

Michael Ghidiu,[a, b] Roman Schlem,[c] and Wolfgang G. Zeier*[c]

Room temperature solution synthesis of electrolytes for all-solid-state batteries has garnered much interest in the past years as a more scalable and efficient alternative to traditional solid-state syntheses. Li_3PS_4, a model solid electrolyte often studied, is typically produced from Li_2S and P_4S_{10}; the latter exists as a molecular solid in an adamantane-like cage structure, and it has been posited that from its robustness arises a rate-limiting reaction step. In this work, we have applied chemistry inspired from the organic thionation literature to easily transform the cage-like P_4S_{10} into more reactive stabilized linear P_2S_5 molecules. This new reagent was used to drastically reduce the synthesis time of Li_3PS_4 in acetonitrile from days to hours. Because the long reaction time of many solvent routes to produce solid electrolytes is considered a bottleneck for commercialization, this work shows great promise for looking toward more fundamental chemistry in order to optimize solution syntheses.

The desire to fully establish all-solid-state batteries, with the ability to maximize energy density by utilizing the lithium metal anode, as a competitor to lithium-ion systems ultimately requires facile scalable production of solid electrolytes with high ionic conductivity.[1,2] The lithium thiophosphates have emerged as viable electrolyte materials due to their high conductivities, acceptable stabilities, and mechanical softness lending to ease of processing.[3,4] One of the more promising synthetic routes in terms of scalability and low energy input involves reacting precursors in solvents to form desired compositions,[5] and also solution-based routes for making precursors themselves.[6] One of the first solution synthesis routes to produce thiophosphate electrolytes formed the β-phase of Li_3PS_4,[7] itself a decent ionic conductor and also an important precursor or intermediate in the production of other thiophosphate compositions such as the argyrodites Li_6PS_5X (X=Cl, Br, I),[8,9] $Li_7P_3S_{11}$,[10,11] and Li_4PS_4I.[12] The reaction to form Li_3PS_4 was first carried out in tetrahydrofuran (THF),[7] but has since been demonstrated in other solvents such as acetonitrile (ACN),[13] ethyl acetate,[14] methyl propionate,[15] mixtures with *N*-methylformamide,[16] and others. The educts are lithium sulfide and readily-available phosphorus pentasulfide; the latter is often referred to as P_2S_5 but in reality exists as the molecular solid P_4S_{10} in an adamantane-like cage structure. This particular structure has been invoked as a potential reason for the typically slow reactions, with the idea that "breaking the cage" is a rate-limiting step that needs to be overcome. Attempts to target this specifically have been made, such as initiation with reactive lithium thioethoxide ($LiSC_2H_5$).[17] It is, however, already known in the organic synthesis literature that P_4S_{10} can be readily reacted with pyridine (abbreviated py) to produce stabilized P_2S_5 as a potent thionating reagent;[18–20] the pyridine adduct stabilizes the otherwise-unfavorable $\sigma^3\gamma^5$ bonding situation of the phosphorus atom.[21] Additionally, it is known that commercial P_4S_{10} contains large amounts of impurities; 20–30% of the total P atoms may be bound in P_4S_9, with S or polysulfidic species making the balance;[22] $py_2P_2S_5$ described above is produced from commercial P_4S_{10} with resulting high purity, so its introduction as an educt should help to alleviate such concerns. Inspired by the need to increase the reaction rate of solvent-synthesized superionic conductors, we set out to introduce pyridine-stabilized P_2S_5 into the solution synthesis of solid electrolytes with the hope of speeding up formation reactions. Using the model system Li_3PS_4, in this work we show its synthesis from the new reagent $py_2P_2S_5$ and Li_2S. A combination of Raman spectroscopy and X-ray diffraction together with electrochemical impedance spectroscopy show a reduction of the reaction time from days to a few hours, resulting in highly pure compounds. We believe this work points to new routes for developing synthesis routes of solid electrolytes for solid state batteries.

As a first step, in order to "break the cage" of P_4S_{10}, a reaction was carried out with pyridine based on the literature (Figure 1a).[21] P_4S_{10} powder, mortared by hand to break up any large particles, was mixed in a flask with pyridine; an immediate reaction was evident; the mixture was stirred for 1 hr and left to rest overnight to promote crystallization of any remaining dissolved products. The resulting powder, collected by filtration and dried, was noticeably less yellow than the starting P_4S_{10}, and the filtrate, which was discarded, was a strong yellow color. We note that since the reaction is conducted in only pyridine, from a commercial perspective, the recovery of the solvent for

[a] Dr. M. Ghidiu
Institute of Physical Chemistry
Justus-Liebig-University Giessen
Heinrich-Buff-Ring 17, 35392 Giessen, Germany
[b] Dr. M. Ghidiu
Center for Materials Research (LaMa)
Justus-Liebig-University Giessen
Heinrich-Buff-Ring 16, 35392 Giessen, Germany
[c] R. Schlem, Prof. W. G. Zeier
University of Münster
Institute for Inorganic and Analytical Chemistry
Corrensstrasse 30, 48149 Münster, Germany
E-mail: wzeier@uni-muenster.de

Supporting information for this article is available on the WWW under https://doi.org/10.1002/batt.202000317

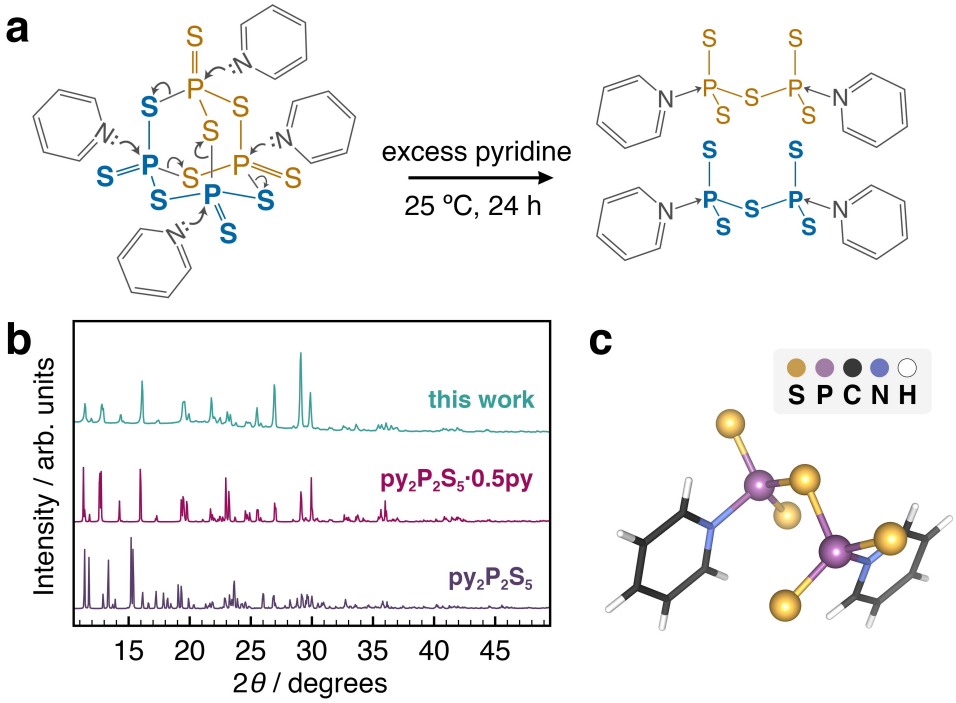

Figure 1. a) Reaction schematic: P_4S_{10} in its typical adamantane-like cage structure reacts with pyridine (py) under mild conditions to form two units of $py_2P_2S_5$, so-called "breaking the cage". The presumed mode of attack by pyridine is illustrated with electron-pushing arrows (note that these are incomplete and only intended to show the attack of pyridine and where the cage splits), and colors illustrating how P_4S_{10} splits. b) XRD of the resulting solid and comparison with the literature. The complex $py_2P_2S_5$ exists in two reported crystal structures: either with,[21] or without,[19] co-crystallized molecules of pyridine. In this case, the reaction yielded the product $py_2P_2S_5 \cdot 0.5py$ (differences in peak intensities are likely due to some degree of texture). c) View of a molecule of $py_2P_2S_5$ from single-crystal diffraction of $py_2P_2S_5 \cdot 0.5py$ by Schönberger *et al.*; the pyridine moieties attached to the phosphorus atoms are perpendicular to the P_2S_5 chains, sticking out of either side, and the N–P bond length is somewhat long at 1.86 Å, suggesting a relatively weak bond.[21]

repeated reactions would be very straightforward. According to previous work, the resulting pyridine-P_2S_5 solvent complex exists in two crystal structures, both triclinic: one with formula $py_2P_2S_5$,[19] and the other co-crystallized with an additional half a molecule of pyridine per formula unit as $py_2P_2S_5 \cdot 0.5py$.[21] Powder X-ray diffraction confirmed that the powders obtained from this reaction were of the latter type (Figure 1b, c). The resulting $py_2P_2S_5 \cdot 0.5py$ has the structure of two corner-sharing trigonal pyramidal PS_3 units, with the pyridine moieties attached to P and on opposite sides of the molecule. Despite how facile the reaction of pyridine with P_4S_{10} to break up the structure is, it has been noted that the coordination between nitrogen and phosphorus of the resulting complex is relatively weak, which should reduce the energy required to remove the pyridine in later steps of synthesis.[21]

For testing this reagent as a replacement of P_4S_{10} for making electrolytes, Li_3PS_4 seemed an obvious model system due to its simplicity, reasonable conductivity, and prevalence in the literature. Acetonitrile (ACN) was chosen as the solvent system because it appears vital to the solution synthesis of $Li_7P_3S_{11}$ (where precipitated Li_3PS_4 is essentially an intermediate),[11] and because the formation of Li_3PS_4 in this solvent is reported in the literature as a rather slow reaction (of the order of days as opposed to $\leq$24 hr in the case of THF),[13] showing much room for improvement. ACN also shows promise for further morphological control of Li_3PS_4, producing plate-shaped crystals.[13,23]

For each synthesis, the solids were simply mixed together mechanically in a mortar and added to a flask, followed by addition of ACN. We found the reaction with $py_2P_2S_5$ to be complete after a period of 4 hours, so this time was chosen as well for the control group synthesis from P_4S_{10}. The precipitates were collected by suction filtration, and any remaining solvent was removed under vacuum at 80 °C. The dried powders were then heat treated for 4 h at 200 °C to remove any solvents complexed to the PS_4^{3-} units.

The reaction with $py_2P_2S_5$ produced a series of color changes: first to a milky suspension with a light yellow tint, then to a white suspension with colorless supernatant, and finally to a very pale greenish-yellow supernatant with fine white precipitates (the initial mixture and the suspension with this final color are shown in Figure S1a). Raman spectroscopy was used to investigate the chemical changes occurring at subsequent treatment steps (Figure 2a). After the initial removal of excess solvent, there was already a strong peak at 418 cm^{-1}, consistent with PS_4^{3-} units, possibly complexed with solvent.[24] There are also two fairly strong peaks at 1003 cm^{-1} and 1034 cm^{-1}; this is not representative of free pyridine (ν_1 and ν_{12} at 991 cm^{-1} and 1030 cm^{-1}) but rather pyridine complexed to Li^+ cations, for instance in zeolites (1002 cm^{-1} and 1036 cm^{-1}).[25] This result suggests that, despite being immersed in excess ACN, pyridine molecules originally bound to the phosphorus atoms of P_2S_5 remain preferentially complexed to the material even after reaction (though likely

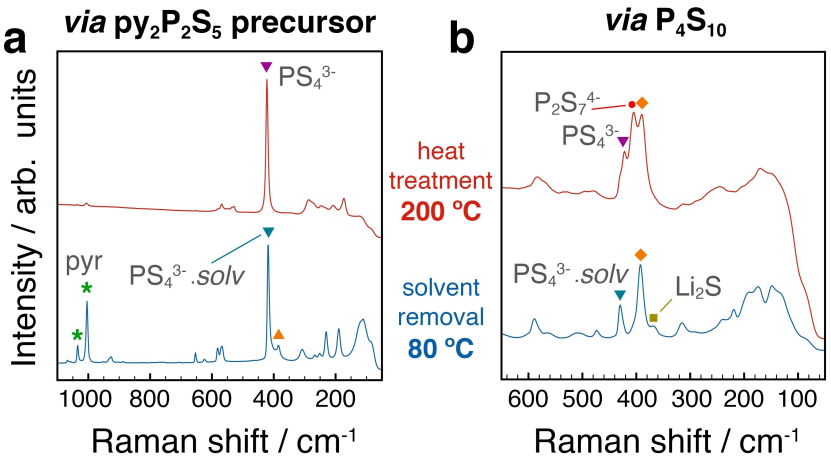

Figure 2. Raman spectroscopy of products after reaction in acetonitrile from Li_2S and a) $py_2P_2S_5 \cdot 0.5py$ or b) standard P_4S_{10}. Measurements were made on dry powders after solvent removal at 80 °C (blue traces, bottom) and subsequently after heat treatment at 200 °C for 4 h (red traces, top). Some features are denoted: solvated PS_4^{3-} units (cyan down triangles, 418 cm^{-1} and 430 cm^{-1}); non-solvent-complexed PS_4^{3-} (purple down triangles, 422 cm^{-1}); $P_2S_7^{4-}$ (red circle, 405 cm^{-1}); Li_2S (yellow square, 369 cm^{-1}); pyridine (green asterisks, 1003 cm^{-1} and 1034 cm^{-1}), possible $P_2S_6^{4-}$ anion (orange up triangle, 385 cm^{-1}), and a potential intermediate phase (orange diamonds, 390–392 cm^{-1}). Figure (b) is truncated as there is no pyridine present, and to show in greater detail the peaks between 300–500 cm^{-1}.

now complexed to Li^+, as demonstrated by Schönberger and coworkers with $py_8Li_4P_2S_6$).[26] There is a small peak at 385 cm^{-1}; this possibly belongs to the undesirable $P_2S_6^{4-}$ anion (to preserve stoichiometry, its formation would require a temporary sink for excess S; PS_4^{3-} units themselves have been suggested as a possibility for this).[27,28] After the 200 °C heat treatment, the pyridine-related peaks disappear and the PS_4^{3-} peak shifts to 422 cm^{-1}, evidence for decomplexation and consistent with other reports of Li_3PS_4.[23] There are no Raman peaks left that can be assigned outside of typical Li_3PS_4. Reactions have been demonstrated in the literature with the explicit intent of breaking the P_4S_{10} cage, but these were carried out with the relatively expensive reagent lithium thioethoxide, 12 h of pre-reaction, an overnight synthesis, and 12 h of heat treatment.[29] In contrast, the reaction time herein is much shorter, and crystals of the pyridine complex are isolated to conclusively demonstrate a breaking of the cage.

The 'standard' route utilizing P_4S_{10} (Figure 2b) showed, after solvent removal, a comparatively small peak at 430 cm^{-1} ascribed to PS_4^{3-} complexed presumably with ACN,[30] most likely unreacted Li_2S at 369 cm^{-1},[31] and a large peak around 392 cm^{-1}, which is potentially an intermediate in the reaction with stoichiometry 1 Li_2S : 1 P_2S_5. Works in the past have noted that mixtures of this stoichiometry (more accurately, 2 Li_2S : 1 P_4S_{10}) are indeed soluble in some organic solvents;[32,33] this would be consistent with this species being a soluble intermediate compared to the otherwise insoluble precursors and product. Another possibility is an ACN/$P_4S_6^{4-}$ complex, suggested from microwave synthesis in acetonitrile; the same combination of peaks around 392 cm^{-1} and 430 cm^{-1} was reported there.[30] After the reaction was ended at 4 hours, the mixture was noticeably yellow compared to the result from the pyridine route above (Figure S1b). After heating to 200 °C, the solvated PS_4^{3-} units now show the typical shift of 422 cm^{-1} in Li_3PS_4, suggesting removal of complexed ACN, but the intensity of this peak is relatively small. There is also some solid-state reaction that produces $P_2S_7^{4-}$ units (405 cm^{-1}). There is a strong peak at 390 cm^{-1} which could correspond to red shifting of the aforementioned peak at 392 cm^{-1}, but this is not certain. All in all it is clear that 4 hours is not enough time for the "standard" route in ACN to produce much PS_4^{3-}.

On a final note concerning the reactions, we found in both syntheses some sensitivity in the ratio of reactants to solvent. The route with P_4S_{10} was carried out with all reactants at 10 wt %; we found that the reaction proved even more sluggish at higher loadings. On the contrary, the reaction with pyridine seemed to proceed more smoothly even at the higher mass loadings, so 20 wt% was used there. This observation could be important, as the mass loading is sometimes not mentioned in reports of solution synthesis.

The structure of the product of the pyridine route after 200 °C was confirmed by X-ray diffraction as the desired high-conducting β-Li_3PS_4 (Figure 3, middle trace, with reference pattern on bottom for comparison). A Rietveld refinement of the diffraction data is shown in the Supporting Information (Figure S2) – the refined orthorhombic structure (space group *Pmna*, $a = 12.9842(5)$ Å, $b = 8.0590(4)$ Å, $c = 6.1373(2)$ Å) showed excellent agreement with β-Li_3PS_4 produced in solution from THF.[7] The standard P_4S_{10} route showed predominately Li_2S reflections (Figure 3, top trace). A much more pronounced Li_2S signal from diffraction as compared to Raman has been noted in the literature.[31] Very weak reflections of β-Li_3PS_4 can be observed; the other signals observed by Raman spectroscopy may be associated with amorphous material and can therefore not be observed here.

To investigate the transport properties of β-Li_3PS_4 obtained by the new pyridine route, temperature dependent AC impedance spectroscopy was performed in the range of −40 °C to 60 °C. Figure 4a shows a representative Nyquist plot of the room temperature measurement, with the orange semicircle

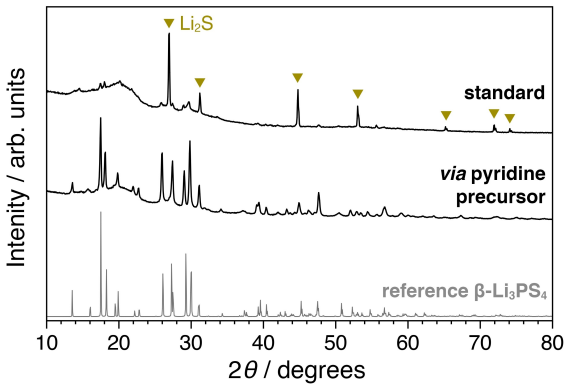

Figure 3. Powder X-ray diffraction of results of the reaction of Li_2S with either standard commercial P_4S_{10} (top) or $py_2P_2S_5 \cdot 0.5py$ (middle) in acetonitrile. The reaction was carried out for 4 h at room temperature, followed by solvent removal at 80 °C (not shown) and heat treatment to 200 °C for 4 h. A reference XRD pattern of β-Li_3PS_4 is provided for comparison (bottom).[7]

being representative for the bulk resistance, with a capacitance of 36 pF cm^{-2} and an α-value of around 0.8. As bulk and grain-boundary contributions cannot be deconvoluted in this temperature range, the Arrhenius diagram in Figure 4b represents the total conductivity. A non-ideal contact between the steel electrodes and the solid electrolyte was furthermore addressed when fitting the blocking tail, with a contribution of 1 µF·cm^{-2}. A conductivity of $2 \cdot 10^{-5}$ S cm^{-1} and activation energy of 0.47 eV were achieved. The conductivity is slightly lower compared to the expected values of ~10^{-4} S cm^{-1} for solution-synthesized Li_3PS_4, but we note that it is much closer to these values than to the roughly 10^{-7} S cm^{-1} which would be expected for standard solid-synthesized β-Li_3PS_4, should it exist at room temperature,[7,34] so the reduction in conductivity here is likely due to a processing issue that can be overcome with further study; it is evident that structurally clean β-Li_3PS_4 is produced. The chemistry of the reaction and its consequences for expanded and rapid syntheses is of great interest here.

We have attempted to improve the rate of reaction for producing Li_3PS_4 as a model electrolyte through targeted chemistry, using pyridine as a reagent to split the common precursor of cage-like P_4S_{10} into more reactive linear molecules. The resulting decrease of reaction time in acetonitrile from days to hours is remarkable, and shows that breaking down P_4S_{10} as a first step can indeed have drastic consequences for the ensuing reaction. This offers new optimization routes for low-energy reactions attractive to industrial production. Further, with the groundwork of this reaction established, there is exciting outlook for tailoring electrolyte production; there are other members of the class of pyridine-stabilized thiophosphates that could potentially be used in targeted syntheses, including $py_2P_2S_7$ (with a bridging S_3 unit between the P atoms) and $py_2P_2S_4O$ (equivalent to the reagent in this work but with a bridging O atom and of possible consequence to the synthesis of mixed S/O Li^+ ion conductors),[21] the anion $pyPS_3^-$,[35,36] and $pyPS_2Cl$.[37] The reagent $py_2P_2S_5$ demonstrated here offers the promise of applicability to all of the solution synthesis routes normally using P_4S_{10} and, since it exists in the crystalline state, could potentially even be used in lower-energy solid-state reactions. This work represents a first step in broadening the chemical routes of solution syntheses for Li^+ ion conducting solid electrolytes.

Acknowledgements

The research was supported by the Federal Ministry of Education and Research (BMBF) within the project FESTBATT under Grant No. 03XP0177A. Open access funding enabled and organized by Projekt DEAL.

Conflict of Interest

The authors declare no conflict of interest.

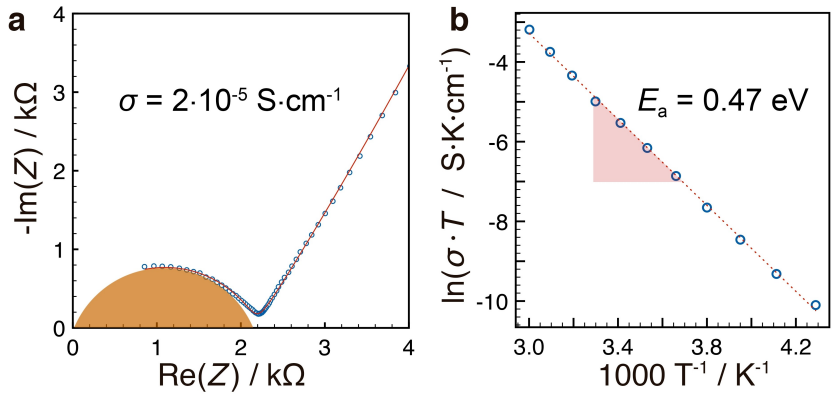

Figure 4. Transport properties of β-Li_3PS_4 synthesized from $py_2P_2S_5$. a) Nyquist plot of impedance measured at 298.15 K. The red trace is a fit, and the orange semicircle represents the bulk resistance, with ionic conductivity of $2 \cdot 10^{-5}$ S·cm^{-1}. b) Arrhenius plot extracted from impedance data measured between −40 and 60 °C. The red trace is a linear least squares fit with activation energy of 0.47 eV extracted from the slope.

Keywords: solid-state battery · thiophosphate · solution synthesis · pyridine · scalable

[1] J. Janek, W. G. Zeier, *Nat. Energy* **2016**, *1*, 1–4.
[2] S. Randau, D. A. Weber, O. Kötz, R. Koerver, P. Braun, A. Weber, E. Ivers-Tiffée, T. Adermann, J. Kulisch, W. G. Zeier, F. H. Richter, J. Janek, *Nat. Energy* **2020**, *5*, 259–270.
[3] K. H. Park, Q. Bai, D. H. Kim, D. Y. Oh, Y. Zhu, Y. Mo, Y. S. Jung, *Adv. Energy Mater.* **2018**, *8*, 1–24.
[4] S. Chen, D. Xie, G. Liu, J. P. Mwizerwa, Q. Zhang, Y. Zhao, X. Xu, X. Yao, *Energy Storage Mater.* **2018**, *14*, 58–74.
[5] M. Ghidiu, J. Ruhl, S. P. Culver, W. G. Zeier, *J. Mater. Chem. A* **2019**, *7*, 17735–17753.
[6] M. Duchardt, M. Diels, B. Roling, S. Dehnen, *ACS Appl. Mater. Interfaces* **2020**, *3*, 6937–6945.
[7] Z. Liu, W. Fu, E. A. Payzant, X. Yu, Z. Wu, N. J. Dudney, J. Kiggans, K. Hong, A. J. Rondinone, C. Liang, *J. Am. Chem. Soc.* **2013**, *135*, 975–978.
[8] S. Yubuchi, M. Uematsu, C. Hotehama, A. Sakuda, A. Hayashi, M. Tatsumisago, *J. Mater. Chem. A* **2019**, *7*, 558–566.
[9] L. Zhou, K.-H. Park, X. Sun, F. Lalere, T. Adermann, P. Hartmann, L. F. Nazar, *ACS Energy Lett.* **2019**, *4*, 265–270.
[10] R. C. Xu, X. H. Xia, Z. J. Yao, X. L. Wang, C. D. Gu, J. P. Tu, *Electrochim. Acta* **2016**, *219*, 235–240.
[11] Y. Wang, D. Lu, M. Bowden, P. Z. El Khoury, K. S. Han, Z. D. Deng, J. Xiao, J. G. Zhang, J. Liu, *Chem. Mater.* **2018**, *30*, 990–997.
[12] S. J. Sedlmaier, S. Indris, C. Dietrich, M. Yavuz, C. Dräger, F. Von Seggern, H. Sommer, J. Janek, *Chem. Mater.* **2017**, *29*, 1830–1835.
[13] H. Wang, Z. D. Hood, Y. Xia, C. Liang, *J. Mater. Chem. A* **2016**, *4*, 8091–8096.
[14] N. H. H. Phuc, M. Totani, K. Morikawa, H. Muto, A. Matsuda, *Solid State Ionics* **2016**, *288*, 240–243.
[15] N. H. H. Phuc, H. Muto, A. Matsuda, *Mater. Today Proc.* **2019**, *16*, 216–219.
[16] S. Teragawa, K. Aso, K. Tadanaga, A. Hayashi, M. Tatsumisago, *J. Mater. Chem. A* **2014**, *2*, 5095.
[17] H. D. Lim, X. Yue, X. Xing, V. Petrova, M. Gonzalez, H. Liu, P. Liu, *J. Mater. Chem. A* **2018**, *6*, 7370–7374.
[18] M. Meisel, H. Grunze, *Z. Anorg. Allg. Chem.* **1968**, *360*, 277.
[19] J. Bergman, B. Pettersson, V. Hasimbegovic, P. H. Svensson, *J. Org. Chem.* **2011**, *76*, 1546–1553.
[20] T. Ozturk, E. Ertas, O. Mert, *Chem. Rev.* **2010**, *110*, 3419–3478.
[21] S. Schönberger, C. Jagdhuber, L. Ascherl, C. Evangelisti, T. M. Klapötke, K. Karaghiosoff, *Z. Anorg. Allg. Chem.* **2014**, *640*, 68–75.
[22] M. C. Démarcq, *Ind. Eng. Chem. Res.* **1991**, *30*, 1906–1911.
[23] Z. D. Hood, H. Wang, A. S. Pandian, R. Peng, K. D. Gilroy, M. Chi, C. Liang, Y. Xia, *Adv. Energy Mater.* **2018**, *8*, 1–7.
[24] N. H. H. Phuc, K. Morikawa, T. Mitsuhiro, H. Muto, A. Matsuda, *Ionics (Kiel).* **2017**, *23*, 2061–2067.
[25] T. A. Egerton, A. H. Hardin, N. Sheppard, *Can. J. Chem.* **1976**, *54*, 586–598.
[26] S. Schönberger, C. Rotter, K. Karaghiosoff, *Heteroat. Chem.* **2014**, *25*, 95–99.
[27] C. Dietrich, D. A. Weber, S. J. Sedlmaier, S. Indris, S. P. Culver, D. Walter, J. Janek, W. G. Zeier, *J. Mater. Chem. A* **2017**, *5*, 18111–18119.
[28] Z. Lin, Z. Liu, W. Fu, N. J. Dudney, C. Liang, *Angew. Chem. Int. Ed.* **2013**, *52*, 7460–7463; *Angew. Chem.* **2013**, *125*, 7608–7611.
[29] H. D. Lim, X. Yue, X. Xing, V. Petrova, M. Gonzalez, H. Liu, P. Liu, *J. Mater. Chem. A* **2018**, *6*, 7370–7374.
[30] K. Suto, P. Bonnick, E. Nagai, K. Niitani, T. S. Arthur, J. Muldoon, *J. Mater. Chem. A* **2018**, *6*, 21261–21265.
[31] Z. W. Seh, H. Wang, P. C. Hsu, Q. Zhang, W. Li, G. Zheng, H. Yao, Y. Cui, *Energy Environ. Sci.* **2014**, *7*, 672–676.
[32] H. Tsukasaki, S. Mori, A. Matsuda, *J. Ceram. Soc. Jpn.* **2018**, *126*, 826–831.
[33] N. H. H. Phuc, A. Matsuda, *Adv. Chem. Res.* **2018**, *42*, 262–272.
[34] R. Kanno, K. Homma, T. Kobayashi, M. Hirayama, M. Yonemura, M. Nagao, *Solid State Ionics* **2010**, *182*, 53–58.
[35] S. Schönberger, Phosphorus, Sulfur and Pyridine, Ludwig-Maximilians-Universität München, **2013**.
[36] A. Dimitrov, I. Hartwich, B. Ziemer, D. Heidemann, M. Meisel, *Z. Anorg. Allg. Chem.* **2005**, *631*, 2439–2444.
[37] M. Meisel, C. Donath, *Z. Anorg. Allg. Chem.* **1983**, *500*, 73–79.

Manuscript received: December 10, 2020
Accepted manuscript online: December 14, 2020
Version of record online: January 5, 2021